Evaluation of the therapeutic efficacy of curcumin nanoparticles in the intestinal and muscular phases of murine trichinosis

Original Article

Noha M Abo-Hussien[1], Shaimaa S Soliman[2], Dina M Sweed[3], Sally S Mandour[4], Noha A Abokhalil[1], Amany F Atia[1]

Departments of Medical Parasitology[1], Public Health and Community Medicine[2], Pathology[3] and Clinical Pathology[4], Faculty of Medicine[1,2], National Liver Institute[3,4], Menoufia University, Shebin El-Kom, Menoufia Governorate, Egypt

ABSTRACT

Background: Curcumin (Cur) exhibits anti-parasitic effects in spite of its poor bioavailability. However, several studies documented use of nanotechnology as efficient drug delivery system.
Objective: To investigate the effect of Cur nanoparticles (Cur-Nano) alone and in combination with albendazole (ABZ) on murine trichinosis.
Material and Methods: A total of 150 laboratory-bred, male Swiss Albino mice were divided randomly and equally into three groups; (I) the intestinal group; (II) the early-treated muscular group; and (III) the late-treated muscular group. Each group was subdivided equally into five subgroups; (a) negative control group; (b) infected non-treated (positive control); (c) mice infected and treated by ABZ; (d) mice infected and treated by Cur-Nano and (e) mice infected and treated by both drugs. Mice were sacrificed on the 7th day post-infection (dpi) (GI) and on the 49th dpi (GII and GIII). The intestinal and muscle specimens were used for H&E, Masson's trichrome, and toluidine blue. Additional study parameters included levels of creatine kinase (CK) to assess degree of muscle destruction, expression levels of vascular endothelial growth factor (VEGF) as well as serum and muscle matrix metalloproteinase 9 (MMP9) to investigate Cur anti-angiogenetic activity, and malonaldehyde (MDA), and total antioxidant capacity (TAC) to determine its anti-oxidant effects.
Results: All treated subgroups showed a significant reduction in adult worm and larval count, with the highest reduction of 99.325 % and 95.94% in GIe and GIIIe respectively. There was a significant improvement in the inflammatory response with significantly decreased expression of VEGF. In both early and late treated mice, serum CK, MDA and MMP9 levels were decreased with improved TAC levels in mice treated with combined treatment and Cur-Nano.
Conclusion: Nanoparticles proved effective drug delivery system for Cur against trichinosis with noticeable outcomes in the muscle phase. The synergistic activity of ABZ/Cur-Nano gives the best results in both intestinal and muscular phases.

Keywords: Albendazole; angiogenesis; anti-inflammatory; antioxidant; curcumin nanoparticles; MMP9, trichinosis; VEGF.

Received: 14 October, 2023; **Accepted:** 4 December, 2023.

Corresponding Author: Noha M. Abokhalil; **Tel.:** +20 1003928052**; Email:** drnoha_abokhalil@yahoo.com

Print ISSN: 1687-7942, **Online ISSN:** 2090-2646, **Vol. 16, No. 3, December, 2023.**

INTRODUCTION

Gastrointestinal nematodes are one of the most common infectious agents in both animals and people, infecting over one billion people globally[1]. Trichinosis in humans is caused by *T. spiralis* that poses a risk to public health and the production of pork and food safety. The disease occurs worldwide and is estimated to cause 10,000 cases each year[2]. Since *T. spiralis* infects a wide range of mammalian hosts, it has frequently been employed as an experimental model to determine the effectiveness of numerous anti-helminthic medications[3]. Human trichinosis occurs through the ingestion of under-cooked or raw meat harboring the infective larvae derived from pigs, horses, and wild omnivorous and/or carnivorous animals[4]. The parasite can be found in the same host in all developmental phases including adults, migratory larvae, and encysted larvae. The presence of adult females in the host's small intestine causes an immune-mediated inflammation with hypersensitivity reaction that is accountable for the underlying intestinal pathology[5].

The mucus layer secreted by the host's intestine serves as the first defense barrier during the infection[6]. When *T. spiralis* causes intestinal inflammation, Th2 responses appear at the time of high worm load, accompanied by a rise in the number of goblet cells, villus atrophy, and crypt hyperplasia[7]. Following delivery by the gravid *Trichinella* female,

 DOI: 10.21608/PUJ.2023.242480.1228

newborn larvae (NBL) migrate directly into the lymphatic and blood vessels of the host. This allows them to reach predilection sites, where they penetrate the highly oxygenated muscles then develop without molting into infective larvae that can survive for years[8]. The invading NBL produce muscle cell damage that activates the satellite cells to undergo proliferation and re-differentiation, thus producing nurse cell and encapsulation of the larvae with the formation of capillary rete[9]. Collagen types I, IV, and VI, the major constituents of the capsule, are synthesized by the nurse cells leading to protection of the larvae from the host immune system[10]. Besides, *T. spiralis* excretory/secretory proteins most likely activate collagen synthesis via the transforming growth factor-β (TGF-β) signaling pathway[11].

De novo angiogenesis generated by trichinosis leads to formation of vascular retes that occurs directly by secreting specific molecules, or by changing the nurse cells in a way that promotes the development of new blood vessels. Trichinosis was found to activate VEGF, a powerful angiogenic stimulator[12]. To continue a sustained host-parasite relationship, *T. spiralis* must remain metabolically active by maintaining proper waste disposal and nutrient acquisition. That is accomplished by attracting the highly permeable vascular retes to the outer surface of the collagen capsule. Therefore, inhibition of angiogenesis may be a suggested mechanism for *T. spiralis* larval developmental suppression[13].

To achieve the optimum results, it is crucial to use potent anthelmintic medications as soon as the intestinal invasion begins. Mebendazole and ABZ are two anthelmintics that are commonly used. However, none are completely effective against the NBL or encysted larvae due to their low absorption, high levels of resistance, and weak action[14]. Recently, there is increasing interest in developing newer effective anti-trichinosis drugs, especially from natural products[3]. Notably, Cur is an extract from the rhizome *Curcuma longa* and has been used since ancient times as a spice, coloring, and flavoring, with a long history in medicine as a bioactive agent. Its pharmacological characteristics, such as its antitumor properties[9], anti-inflammatory, and anti-microbial effects may make it beneficial. Additionally, Cur has antioxidant effects[15]. It is considered as a very potent lipid-soluble antioxidant because it can transform the lipid radicals in the cell membrane into phenoxyl radicals. Changes in MDA and TAC levels are useful indicators for assessing the oxidative stress[16].

Moreover, several reports showed that Cur can act as an antiparasitic agent. It was active against *G. intestinalis, Leishmania* spp., *T. cruzi, T. evansi, C. parvum*, and *T. gondi*[17]. It also had a significant effect on the progression of experimental cerebral malaria, where treated mice survived longer after receiving treatment, and cerebral malaria either didn't develop or didn't progress[18].

Despite being a powerful bioactive agent and natural antioxidant, Cur use is limited due to its poor water solubility, fast degradation, and low bioavailability. Nanotechnology can solve this problem by rendering it water-soluble thus enhancing its activity against various microbial pathogens and parasites. Several studies used Cur-Nano on a wide scale as delivery systems for medications or vaccinations, to increase their therapeutic efficacy, and to enhance the bioavailability of therapeutic agents and bioactive compounds[15,19,20]. This study aimed to evaluate the effects of Cur-Nano, either alone or in combination with ABZ on *T. spiralis*-infected mice in the intestinal and muscular phases of trichinosis.

MATERIAL AND METHODS

This experimental case-control study was conducted in Medical Parasitology Department, Faculty of Medicine, Menofia university; National Liver Institute, Menofia university, and Theodore Bilharz Research Institute (TBRI), During the period from 6/2022 to 6/2023.

Study design: The study included three groups of mice: GI (intestinal), GII (early treated muscular) and GIII (late treated muscular). Each group was further subdivided into five subgroups according to the drug used. Mice of all subgroups were subjected to parasitological, histopathological, immunohistochemical, biochemical, and anti-oxidants parameters assessment to evaluate the effect of Cur-Nano and ABZ.

Animals: One hundred and fifty laboratory-bred, parasite-free, Swiss Albino male mice, 7-10 weeks old and weighing ~18-20 g, were used. Mice were acquired from Theodore Bilharz Research Institute's (TBRI) animal facility in Giza, Egypt. Mice were kept under controlled conditions of temperature (25±2°C), humidity (70%) and lighting. They had unlimited access to standard pellet diet and water.

Parasites: *T. spiralis* larvae were originally obtained from the European Union Reference Laboratory for Parasites, Superior Institute of Health, Rome, Italy, where they were genotyped as *T. spiralis*. The larvae were kindly provided from the maintained strain by repeated passes through rats and mice at the Medical Parasitology Department, Tanta University, Egypt. Before the study, to ensure that mice were clear of any intestinal parasite infections, a stool examination was performed.

Experimental groups and subgroups: One hundred and fifty mice were divided randomly and equally into three main groups; each includes 50 mice. Group I (GI)

is the intestinal group that was subdivided equally into five subgroups (ten mice each), subgroup Ia;, non-infected non-treated (negative control), subgroup Ib; infected non-treated (positive control), subgroup Ic; mice infected and treated by ABZ, subgroup Id; mice infected and treated by Cur-Nano and subgroup Ie; mice infected and treated by both drugs (Cur-Nano/ ABZ). Similarly, groups II, and III, the muscular early, and late treated groups, were subdivided equally into five subgroups.

Mice infection: Each mouse received oral infection with 200 *T. spiralis* larvae using an intra-esophageal tube[19].

Drugs and dosage: Albendazole was purchased as Alzental (Epico, Cairo, Egypt). One tablet (100 mg) was dissolved in 50 ml of distilled water and was given orally at a dose of 50 mg/kg/d for three days[3]. Curcumin nanoparticles were created using the process of solvent-antisolvent precipitation[21]. Briefly, ethanol (Vetec, 99.8%) was used to dissolve Cur (100 mg/ml). Distilled water was added as an antisolvent at a ratio of 1:10 and thoroughly mixed, for ~30 min sonication. The sonicating mixture was agitated at 800 rpm for roughly 20 min to produce an orange-colored precipitate. It was maintained at 25°C to 40°C under a nitrogen atmosphere and high pressure to reach 0.1% to 10%. The particle size of Cur-Nano was determined using the Horiba SZ-100 (Japan) particle size analyzer. Atia *et al*.[22] utilized Cur-Nano at a dose of 50 mg/kg orally for five days, noting a 90.85% parasite inhibition at this dose. In the combination treatment (Cur-Nano/ ABZ), the same dose was used.

Dosage schedule: For GI (intestinal group), the treatment started on the 3rd dpi for three consecutive days and mice were sacrificed on the 7th dpi[23], to evaluate the effect of the drug against the adults. To evaluate the effect of the drugs during the muscle phase, treatment started on the 13th dpi for GII (early treated group)[24] and on the 31st dpi for GIII (late treated group)[19]. Mice scarification for muscle phase groups (GII and GIII) was carried on the 49th dpi[25].

Scarification and sample collection: Mice were euthanized by cervical dislocation on the 7th dpi (GI) and the 49th dpi (GII and GIII). Blood samples (2 ml) were collected, left at room temperature for 30 min and centrifuged for 15 min at 3000 rpm. The serum was kept at -20°C for further quantitative estimation of CK, MMP9, MDA, and TAC levels. The whole small intestine (of GI subgroups) and muscle tissues from togue and diaphragm (of GII and GIII subgroups) were excised and preserved in neutral buffered formalin (pH 7.2) for additional H&E and immunohistochemical (IHC) stains.

Intestinal adult load: To encourage the worms to move out of the tissue and gather in the container, the washed intestinal samples from GI mice were chopped into small pieces (1 cm each) and incubated at 37°C in a 250 ml beaker containing 100 ml of Hanks' balanced salt solution for 2 h. After pipetting the solution, saline was used to repeatedly cleanse the gut. The total fluid was gathered in tubes and centrifuged for five min at 1500 rpm. The sediment was reconstituted in 3-5 drops of saline for worm counting, and then it was microscopically examined (X10) drop by drop[26] using the following equation: Efficacy of treatment (%) = 100 X mean number (No) of adults recovered in control - mean No recovered in treated mouse/mean No of adults recovered in control[27].

Muscular larva load: According to Nassef *et al*.[19], each mouse of GII and GIII was dissected and digested in 1% pepsin (1:10.000) and 1% concentrated hydrochloric acid (HCL) in 200 ml distilled water. An electric stirrer was used to continuously agitate the mixture for one hour at 37°C. To get rid of the large particles, the digested product was run through a sieve with a mesh size of 50/inch. The encysted larvae were gathered on a sieve with a mesh size of 200/inch, rinsed twice with tap water, and then suspended in 150 ml of tap water in a conical flask. Afterwards, the supernatant liquid was removed, and a McMaster counting chamber was used to count the sediment larvae under a microscope[28] using the following equation: Treatment effectiveness (%) = 100 x mean No recovered in the control - mean No recovered covered in treated mice/mean No recovered in the control[27].

Histopathological study: Specimens from the small intestine, tongue, and diaphragm were collected from the sacrificed mice of all groups. All specimens were fixed in neutral buffered formalin (pH 7.2), embedded in paraffin blocks, and sliced at 4-5 µm tissue thickness. Methods of staining were based on the staining protocols of Bancroft and Gamble[29].

- **Ordinary H&E staining** was used to assess the enteropathy and inflammatory response during the intestinal phase, and the presence of larva and the degenerative inflammatory response in the muscle phases. During the intestinal phase, the stained slides were assessed for the severity of enteropathy as follows: epithelial hyperplasia graded as absent (0), mild (1), moderate (2), and severe (3). The severity of inflammation (0–4) is defined as; no significant inflammation (0), mild cellular infiltrate within the lamina propria (1), moderate (2), severe and extending into the submucosa (3); and severe with crypt abscess, goblet cell depletion, and ulceration (4)[30]. In all cases, the inflammatory cell types were counted in 15 villous-crypts units selected at a higher power magnification (400×). Eosinophils have a characteristic red granule on the H&E stain. The final score was calculated as the mean of cells ± standard deviation (SD)[31]. To assess the severity of inflammatory infiltrate around the larva during the muscle phase, twenty non-overlapping representative

high-power fields (40x) of H&E-stained slides were examined for the No and size of larvae, the status of the capsule, the integrity of the internal structure, necrosis, and lysis. The effect of trichinosis on the infected skeletal muscle was assessed based on the loss of striations, central nuclei, and vacuolations[11,32].

- **Masson trichrome (MT) stain** was performed to assess collagen deposition in the muscles infected by *T. spiralis*. Briefly, slides were stained by Weigert's iron hematoxylin working solution for 10 min, washed, and stained with Biebrich scarlet-acid fuchsin solution for 15 min. The slides were re-washed, followed by dipping in phosphomolybdic-phosphotungestic acid solution for 15 min then transferred directly to aniline blue solution for 10 min. Slides were rinsed briefly in distilled water followed by 1% acetic acid solution for 5 min. The collagen fibers stained blue against red-stained muscle fibers. According to Cheng *et al*.[33], *Trichinella* capsule thickness was subjectively categorized as mild, moderate, and marked.
- **Toluidine blue stain** was used to better visualize the inflammatory cells in the intestinal specimen. Toluidine blue (0.04%) in 0.1 M sodium acetate buffer (pH 4) stain mast cells violet or red purple. The stain was evaluated as either negative or positive, and mast cells were counted using x20[34]. Microscopy and image capture were performed with an Olympus CX41 microscope and DP26 camera, Shinjuku, Tokyo, Japan.

Immunohistochemical studies: The immunostaining technique was done using the streptavidin-biotin system[35]. The primary antibodies used were MMP 9 diluted as 1:300 (Cat. #13667) and VEGF diluted as 1:500 (Cat. #2479) obtained from Cell Signaling Technology, Massachusetts, USA. The tissue was deparaffined and rehydrated followed by antigen retrieval using high pH EDTA solution for 20 min, then cooling at room temperature for an additional 20 min. The primary antibodies were applied to each slides overnight at 4°C. A secondary antibody using Ultravision detection system anti-polyvalent HRP/DAB, ready-to-use, Neomarker, was applied and staining was visualized using DAB chromogen substrate and Mayer's hematoxylin as a counterstain. In each run, positive and negative controls were included. Positive expression of VEGF and MMP 9 antibodies showed cytoplasmic localization. The expression was assessed using Histoscore (H score) and calculated by multiplying the intensity and percent of cells as follows (strong intensity (3) x percentage) + (moderate intensity (2) x percentage) + (mild intensity (1) x percentage) + (negative staining (0) x percentage). A final score was obtained at a range of 0-300[36].

Creatine kinase: Measurement of total CK serum levels was performed using a CK reagent kit for serum and plasma (Beckman Coulter, CA, USA) with a linear range from 5 to 1200 U/l (0.1–20.0 mkat/l)[37].

Matrix metalloproteinase: Serum concentrations of MMP were measured using ELISA kits (Daiichi Fine Chemical Co. Ltd., Toyama, Japan). Calibrators and samples were incubated together with anti-MMP monoclonal antibodies in microstrips. After washing, 90 µl buffered substrate/chromogen reagent was added to each sample, and the enzyme reaction was allowed to proceed. Reaction color was changed as a result of the enzyme reaction, the intensity of which was proportional to the amount of MMP present in the samples. The MMP concentrations in samples were then read from a calibration curve[38].

Malonaldehyde: The chemicals were bought from Merck (Germany), Scharlau (Spain), and Sigma-Aldrich (St. Louis, USA). By calculating the byproducts of the reaction between MDA and thiobarbituric acid (TBA), serum MDA concentrations were calculated according to Malik *et al.*[39]. By adding 20% trichloroacetic acid solution containing 8.1% Sodium dodecyl sulfate (SDS) and 0.8% aqueous solution TBA to 50 µl serum, the reaction products between MDA and TBA were isolated. The mixture was heated up for one hour in a boiling water bath and then cooled on ice. The mixture was then incorporated with N-butanol, and it was centrifuged for 10 min at 4000 rpm. The organic layer was taken and read at 532 nm to distinguish the reaction products. To prepare the standards, 1,1,3,3-tetraethoxy propane was employed.

Total antioxidant capacity: The ferric reducing antioxidant power assay (FRAP) was used for estimating TAC. This method is based on the reduction of Fe^{3+} to Fe^{2+} due to the action of antioxidants[40]. Briefly, 900 µl of freshly prepared FRAP (37°C) working reagent (300 mM/L acetate buffer (pH 3.6), with 10 mM 2,4,6-tri(2-pyridyl)-1,3,5-triazine solution in 40 mM HCl, and 20 mM $FeCl_3$ solution in a ratio of 10:1:1 respectively) was added to 100 µl of serum (previously diluted with distilled water 1:1) and then incubated for 25 min at 37°C. The reaction absorbance was determined by a spectrophotometer at 593 nm, using different known concentrations of $FeSO_4.7H_2O$ in a range of 0.2 to 1 mM/L to prepare a standard curve.

Statistical analysis: The SPSS statistical package version 23 was used to tabulate and statistically analyze the raw data (SPSS Inc. Released 2015. IBM SPSS Statistics for Windows, version 23.0, Armnok, NY: IBM Corp). Number (No), percentage (%), mean ($\bar{x}$), and standard deviation (SD) were used to express our data. After determining if the data were homogeneous, the Kruskal-Walli's test and Tamhane's test were employed to compare quantitative variables between more than two groups. For the comparison of quantitative variables between two groups, Mann-Whitney's test was employed. The relationship between qualitative variables was investigated using

the chi-square (χ^2) test (together with the *Z* test to compare column percentage). Fischer's Exact test was employed whenever any of the predicted cells fell below the threshold of five. Statistical significance was defined with a two-sided $P<0.05$.

Ethical consideration: The ethical committee of Faculty of Medicine, Menoufia University, Egypt, approved the housing and feeding of mice in accordance with national regulations (IRB; PARA11).

RESULTS

Drug effects on mature worms: The intestinal subgroup GIe had significantly the lowest worm count and the highest reduction rate (1.10±1.52, and 99.325%, respectively) followed by subgroup Ic (10.20±1.93, and 93.80% respectively), and subgroup Id (46.40±3.77, and 71.80%, respectively), while subgroup GIb (positive control) had the highest count (164.80±5.76). All the subgroups were significantly different when compared to each other (Table 1).

Effects on encysted larvae: Among the early treated muscular subgroups, GIIe had significantly the lowest larval count and the highest reduction rate (6890.70±478.77, and 89.11% respectively) followed by GIIc (16260±627.51, and 74.34% respectively), then GIId (22260.00±627.51, and 64.88%, respectively), while in GIIb, the larval count was 63390.00±3165.94. All the subgroups were significantly different from each other (Table 1). Similarly, in the late treated muscular group (GIII), the lowest larval count and the highest reduction rate (2789.4±284.14, and 95.94%, respectively) was in GIIIe followed by GIIId (10135.0±259.83, and 85.26%, respectively) and lastly subgroup GIIIc (20267.60±406.48, and 70.51%, respectively) (Table 1).

Comparing the efficacy of treatment in the muscle phase in relation to the day of administration, statistically significant changes with marked larval elimination were found when the Cur-nano/ABZ or Cur-Nano were administered on the 31st dpi (late treatment) in GIIIc and GIIIb, respectively. Lower results were recorded with early treatment on 13th dpi (GIIe and GIId, respectively). On the other hand, in the ABZ-treated subgroups; the early treated GIIc showed better eradication of larvae than the late treated subgroup GIIIc (Table 1).

The histopathological changes of the intestinal phase *T. spiralis*: By H&E staining, a significant enteropathy was observed in the *T. spiralis* infected non-treated subgroup GIa compared to the treated subgroups; (GIc, GId and GIe) in the form of a marked decrease in villous/crypt ratio, crypt hyperplasia and goblet cell depletion (Fig. 1a, b). ABZ-treated (GIc) and Cur-Nano/ABZ treated (GIe) subgroups showed a similar significant improvement of the inflammatory response in the form of restoration of the villous/crypt ratio and goblet cells ($P<0.001$) (Fig. 1d, j). However, the improvement was limited in the Cur-Nano treated subgroup (Gid) that exhibited moderate villous/crypt blunting and goblet cell depletion (Fig. 1g). Similarly, the score of inflammatory cells significantly declined to score 1 in GIc and GIe, while decreasing to score 2 in the Cur-Nano treated subgroup GId ($P<0.001$) (Fig. 1e, h, k).

By toluidine blue staining, the load of eosinophils considerably decreased in the treated subgroups compared to the infected non-treated subgroup GIa (mean ±SD, 79.70±4.08) ($P<0.001$, for all). The eosinophils count significantly declined in GIe (17.40±2.41), followed by GIc (19.50±0.70) compared to GId (29.10±0.87), with P<0.001 for both. Similarly, the mast cells count considerably decreased in all

Table 1. The mean worm and larval count among different subgroups.

Intestinal groups	Worm count	Reduction rate%	Statistical analysis	
	Mean ± SD		*P* value	Post Hoc
GIb	164.8 ± 5.76			
GIc	10.2 ± 1.93	93.80	<0.001	*P*1<0.001, *P*2<0.001, *P*3<0.001, *P*4<0.001, *P*5<0.001, *P*6 <0.001
GId	46.4 ± 3.77	71.80		
GIe	1.1 ± 1.52	99.325		
Muscular groups	**Larval count**	**Reduction rate%**	**Statistical analysis**	
	Mean ± SD		***P* value**	**Post Hoc**
GIIb	63390.0 ± 3165.94			
GIIc	16260.0± 627.51	74.34	<0.001	*P*1<0.001, *P*2<0.001, *P*3<0.001, *P*4<0.001, *P*5<0.001, *P*6 <0.001
GIId	22260.0 ± 627.51	64.88		
GIIe	6890.7 ± 478.77	89.11		
GIIIb	68800.0 ± 2245.98			
GIIIc	20267.6 ±406.48	70.51	<0.001	*P*1<0.001, *P*2<0.001, *P*3<0.001, *P*4<0.001, *P*5<0.001, *P*6 <0.001
GIIId	10135.0 ± 259.83	85.26		
GIIIe	2789.4 ± 284.14	95.94		

***P*1:** b Vs c, ***P*2:** b Vs d, ***P*3:** b Vs e, ***P*4:** c Vs d, ***P*5:** c Vs e, ***P*6:** d Vs e.

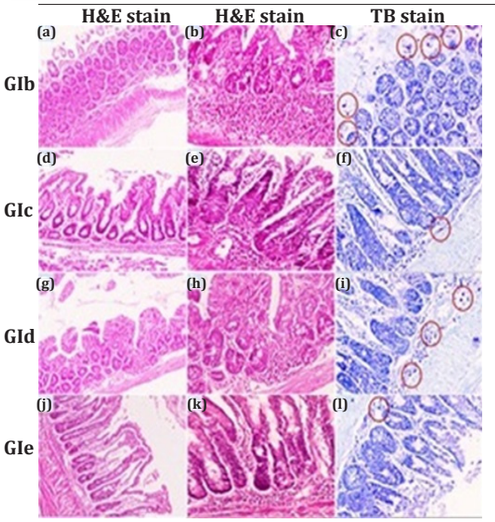

Fig. 1. The histopathological changes in the intestinal phase of trichinosis in the studied subgroups. **a)** Marked decrease villous/crypt ratio and crypt hyperplasia in the infected subgroup (H&E x40). **b)** Marked inflammatory infiltrate in infected subgroup (H&E x100). **c)** Prominent mast cells between the intestinal crypts in infected subgroup (TB x100). **d)** Mild villous atrophy and crypt hyperplasia in ABZ-treated subgroup (H&E x40). **e)** Mild inflammatory infiltrate in ABZ-subgroup (H&E x100). **f)** Low number of mast cells between the intestinal crypts in ABZ-treated subgroup (TB x100). **g)** Moderate villous atrophy and crypt hyperplasia in Cur-Nano treated subgroup (H&E x40). **h)** Moderate inflammatory infiltrate in Cur-Nano treated subgroup (H&E x100). **i)** Moderate number of mast cells between the intestinal crypts in Cur-Nano treated subgroup (TB x100). **j)** Mild villous atrophy and crypt hyperplasia in ABZ/Cur-Nano treated subgroup (H&E x40). **k)** Mild inflammatory infiltrate in ABZ/Cur-Nano treated subgroup (H&E x100). **l)** Low number of mast cells between the intestinal crypts in ABZ/Cur-Nano treated subgroup (TB x100). **TB:** Toluidine blue staining.

Table 2. The histopathological changes during the intestinal phase in the studied groups subgroups.

Variable	Subgroups				Statistical analysis
	GIb	GIc	GId	GIe	
	No. (%)	No. (%)	No. (%)	No. (%)	*P* value
Epithelial hyperplasia					
Mild	0 (0.0)†	7 (70.0)*	2 (20.0)	7 (70.0) *	<0.001
Moderate	0 (0.0)†	3 (30.0)	8 (80.0)*	3 (30.0)	
Marked	10 (100.0)*	0 (0.0)	0 (0.0)	0 (0.0)	
Inflammation					
Mild	0 (0.0)†	7 (70.0)*	2 (20.0)	8 (80.0) *	<0.001
Moderate	0 (0.0)†	3 (30.0)	8 (80.0)*	2 (20.0)	
Marked	10 (100.0)*	0 (0.0)	0 (0.0)	0 (0.0)	
Goblet cell depletion					
Mild	0 (0.0)†	9 (90.0)	8 (80.0)	10 (100.0)*	<0.001
Moderate	0 (0.0)	1 (10.0)	2 (20.0)	0 (0.0)	
Marked	10 (100.0)*	0 (0.0)	0 (0.0)	0 (0.0)	
Villous/crypt ratio					
Mild	0 (0.0)†	7 (70.0)*	2 (20.0)	7 (70.0)*	<0.001
Moderate	0 (0.0)†	3 (30.0)	8 (80.0)*	3 (30.0)	
Marked	10 (100.0)*	0 (0.0)	0 (0.0)	0 (0.0)	

Variable	Subgroups				Statistical analysis	
	GIb	GIc	GId	GIe		
	Mean±SD	Mean±SD	Mean±SD	Mean±SD	*P* value	Post Hoc
Eosinophil	79.7±4.08	19.5±0.70	29.1±0.87	17.4±2.41	<0.001	*P*1<0.001, *P*2<0.001, *P*3<0.001, *P*4 <0.001, *P*5 0.134, *P*6 <0.001
Mast cell	28.1±1.96	3.3±0.82	16.5±0.84	1.2±0.42	<0.001	*P*1 <0.001, *P*2 <0.001, *P*3 <0.001, *P*4 <0.001, *P*5 <0.001, *P*6 <0.001

***:** Significantly higher than their corresponding in the other subgroups; **†:** Significantly lower than their corresponding in the other subgroups; ***P*1:** b Vs c, ***P*2:** b Vs d, ***P*3:** b Vs e, ***P*4:** c Vs d, ***P*5:** c Vs e, ***P*6:** d Vs e.

treated subgroups compared to infected non-treated GIa (28.10±1.96) with P<0.001, for all subgroups. Mast cells count was significantly reduced in GIe (1.20±0.42), followed by GIc (3.30 ± 0.82) and GId (16.50 ± 0.84) and *P*<0.001 for all subgroups (Fig. 1c, f, i, l, and table 2).

The histopathological changes of the early treated muscle phase groups (treatment on the 13th dpi): The mean number of larvae was significantly decreased in GIIe 16.80±1.22), followed by GIIc (19.80±1.75) and GIId (33.20±9.30) compared to GIIb (64.90±12.07) (Table 3). In addition, by H&E staining, there was significant thinning of the capsule, degradation of the internal structures, and lysis of the larva in all treated subgroups compared to the *T. spiralis* infected non-treated subgroup (*P*<0.001). The response was better observed in the Cur-Nano/ABZ treated subgroup (GIIe) followed by ABZ-treated (GIIc) and then Cur-Nano treated subgroup (GIId) (Fig. 2 a, d, g, j). Similarly, the inflammatory response around larvae was significantly

declined in GIIe followed by GIIc and GIId compared to GIIb (P<0.001) (Fig. 2 b, e, h, k).

By Masson trichrome staining, the muscle degenerative changes were significantly decreased in all treated subgroups compared to the infected non-treated subgroup. Moreover, improvement in the form of maintained striations, peripheral nuclei, and less collagen deposition was significantly observed in GIIe compared to either GIIc or GIId (P=0.025) (Fig. 2 c, f, i, l).

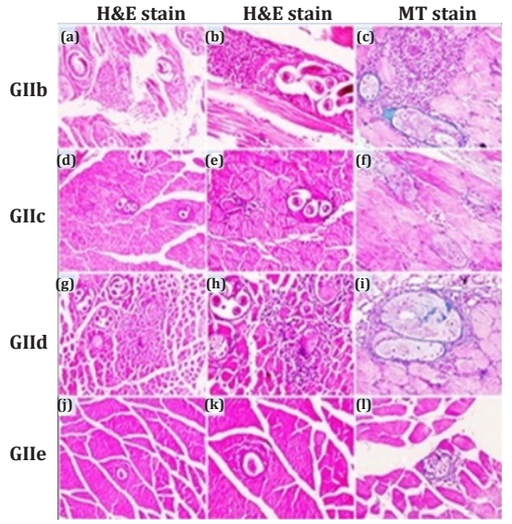

Fig. 2. The histopathological changes in the early treated muscular phase in the studied subgroups. a) Marked dense infiltrate by *T. spiralis* larvae in the infected subgroup (H&E x40). b) Marked inflammatory infiltrate with little destruction of the larva in the infected subgroup (H&E x100). c) Thick capsule around the larva in the infected subgroup (MT x100). d) Low number and size of *T. spiralis* larva in ABZ-treated subgroup (H&E x40). e) Mild inflammatory infiltrate associated with marked lysis of the larva in ABZ-treated subgroup (H&E x100). f) Thinning of the larval capsule in ABZ-treated subgroup (MT x100). g) Moderate number of *T. spiralis* larva infiltration in Cur-Nano treated subgroup (H&E x40). h) Moderate inflammatory infiltrate with mild lysis of the larva in Cur-Nano treated subgroup (H&E x100). i) Mild thinning of the capsule of *T. spiralis* larva in Cur-Nano treated subgroup (MT x100). j) Few numbers of *T. spiralis* larval infiltration in ABZ/Cur-Nano treated subgroup (H&E x40). k) Minimal inflammatory infiltrate and marked lysis of larva in ABZ/Cur-Nano treated subgroup (H&E x100). l) Marked thinning of larval capsule in ABZ/Cur-Nano treated subgroup (MT x100). **MT:** Masson trichrome.

Table 3. The histopathological changes during the early treated muscle phase in the studied subgroups.

Variable	Early treated muscle subgroups				Statistical analysis
	GIIb No. (%)	GIIc No. (%)	GIId No. (%)	GIIe No. (%)	*P* value
Inflammation					
Mild	0 (0.0)†	7 (70.0)*	2 (20.0)	9 (90.0)*	<0.001
Moderate	7 (70.0)*	3 (30.0)†	8 (80.0)*	1 (10.0)†	
Marked	3 (30.0)†	0 (0.0)	0 (0.0)	0 (0.0)	
Capsule thinning					
Absent	10 (100.0)*	0 (0.0)	0 (0.0)	0 (0.0)	<0.001
Mild	0 (0.0)	2 (20.0)	8 (80.0)*	0 (0.0)	
Moderate	0 (0.0)†	8 (80.0)*	2 (20.0)	2 (20.0)	
Marked	0 (0.0)	0 (0.0)	0 (0.0)	8 (80.0)*	
Degradation					
Absent	10 (100.0)*	0 (0.0)	0 (0.0)	0 (0.0)	<0.001
Mild	0 (0.0)	2 (20.0)	9 (90.0)*	0 (0.0)	
Moderate	0 (0.0)†	8 (80.0)*	1 (10.0)	1 (10.0)	
Marked	0 (0.0)	0 (0.0)	0 (0.0)	9 (90.0)*	
Muscle by MT					
Mild	0 (0.0)†	4 (40.0)	4 (40.0)	6 (60.0)	<0.001
Moderate	10 (100.0)*	6 (60.0)	6 (60.0)	4 (40.0)	

Variable	Subgroups				Statistical analysis	
	GIIb Mean±SD	GIIc Mean±SD	GIId Mean±SD	GIIe Mean±SD	*P* value	Post Hoc
No. of larva	64.9±12.07	19.8±1.75	33.2±9.30	16.8±1.22	<0.001	*P*1<0.001, *P*2<0.001, *P*3<0.001, *P*4<0.001; *P*5=0.30, *P*6<0.001
Eosinophil	39.8±0.91	18.8±0.91	31.9±2.64	4.8±0.78	<0.001	*P*1<0.001, *P*2<0.001; *P*3<0.001, *P*4<0.001; *P*5<0.001, *P*6<0.001
Mast cell	8.3±3.52	3.7±1.56	4.0±3.62	2.6±2.22	<0.001	*P*1<0.001, *P*2=0.002, *P*3<0.001, *P*4=0.817, *P*5=0.397, *P*6=0.283
VEGF	131.5±81.31	31.5±36.28	40.5±38.67	19.0±22.94	<0.001	*P*1=0.022, *P*2=0.050, *P*3=0.010, *P*4=0.998, *P*5=0.938, *P*6=0.790
MMP9	161.0±87.87	71.0±67.12	52.5±47.16	45.0±25.82	0.001	*P*1=0.772, *P*2<0.001, *P*3<0.001, *P*4=0.475, *P*5=0.317, *P*6<0.001

***:** Significantly higher than their corresponding in the other subgroups; **†:** Significantly lower than their corresponding in the other subgroups; ***P*1:** b Vs c, ***P*2:** b Vs d, ***P*3:** b Vs e, ***P*4:** c Vs d, ***P*5:** c Vs e, ***P*6:** d Vs e.

Regarding the inflammatory cellular subtype, the eosinophils count significantly declined in all treated subgroups compared to the infected non-treated subgroup (39.80±0.91) with *P*<0.001 for all subgroups. The eosinophils count was significantly low in GIIe (4.80±0.78), followed by GIIc (18.80±0.91) and then GIId (31.90±2.64) (*P*<0.001 for all). Similarly, the mast cells count significantly decreased in GIIe (2.60±2.22), GIIc (3.70±1.56), and GIId (4.0±3.62) compared to GIIb (8.30±3.52) (*P*<0.001, *P*=0.001 and *P*=0.002, respectively). However, there was no significant difference between ABZ, Cur-Nano, and Cur-Nano/ABZ treated subgroups regarding mast cells count (Table 3).

The histopathological changes of the late treated muscle phase (treatment on the 31st dpi) in the studied subgroups: The number of larvae was significantly decreased in the Cur-Nano/ABZ treated GIIIe (10.70±1.56), followed by Cur-Nano treated GIIId (18.80±1.22) and ABZ-treated GIIIc (24.20±6.40) compared to *T. spiralis* infected non-treated group GIIIb (61.90±6.87) (Table 4).

By H&E staining, there was significant thinning of the capsule, degradation of internal structures, and lysis of the larvae in all treated subgroups compared to the positive control subgroup GIIIb (*P*<0.001). The response was best observed in GIIIe compared to GIIIc and GIIId (both showed similar degrees of larval degeneration and lysis). The inflammatory response around larvae was significantly declined in all treated subgroups compared to the infected non-treated subgroup (*P*<0.001) (Fig. 3 a, d, g, j). The inflammation was mild in GIIIe followed by GIIId and then GIIIc (Fig. 3 b, e, h, k).

By Masson trichrome staining, the muscle degenerative changes were significantly decreased in the treated subgroups compared to the infected non-treated subgroup (*P*<0.001) (Fig. 3 c, f, i, l). The improvement was significantly observed in GIIIe and GIIId compared to GIIIc (Table 4).

Regarding the inflammatory cellular subtype, the eosinophils count considerably decreased in all

Table 4. The histopathological changes during the late treated muscle phase in the studied subgroups.

Variable	Late treated muscle subgroups				Statistical analysis
	GIIIb No. (%)	GIIIc No. (%)	GIIId No. (%)	GIIIe No. (%)	*P* value
Inflammation					
Mild	0 (0.0)	3 (30.0)†	7 (70.0) *	10 (100.0) *	<0.001
Moderate	2 (20.0)	7 (70.0)*	3 (30.0) †	0 (0.0)	
Marked	8 (80.0)*	0 (0.0)	0 (0.0)	0 (0.0)	
Capsule thinning					
Absent	10 (100.0) *	0 (0.0)	0 (0.0)	0 (0.0)	
Mild	0 (0.0)	0 (0.0)	0 (0.0)	0 (0.0)	<0.001
Moderate	0 (0.0) †	6 (60.0)*	6 (6.0)	2 (20.0)†	
Marked	0 (0.0) †	4 (40.0)	4 (40.0)	8 (80.0)*	
Degradation					
Absent	10 (100.0) *	0 (0.0)	0 (0.0)	0 (0.0)	
Mild	0 (0.0)	0 (0.0)	0 (0.0)	0 (0.0)	<0.001
Moderate	0 (0.0) †	6 (60.0)	5 (50.0)	3 (30.0)†	
Marked	0 (0.0) †	4 (40.0)	5 (50.0)	7 (70.0)*	
Muscle by MT					
Mild	0 (0.0)	3 (30.0)	8 (80.0) *	10 (100.0)*	<0.001
Moderate	0 (0.0)	7 (70.0)*	2 (20.0)	0 (0.0)	
Marked	10 (100.0) *	0 (0.0)	0 (0.0)	0 (0.0)	

Variable	Subgroups				Statistical analysis	
	GIIb Mean±SD	GIIc Mean±SD	GIId Mean±SD	GIIe Mean±SD	*P* value	Post Hoc
No. of larva	61.9± 6.87	24.2±6.40	18.8±0.22	10.7±1.56	<0.001	*P*1<0.01, *P*2<0.001, *P*3<0.001, *P*4=0.06, *P*5<0.001, *P*6<0.001
Eosinophil	51.9± 3.07	21.2±1.39	14.8±0.91	10.0±0.66	<0.001	*P*1<0.001, *P*2<0.001, *P*3<0.001, *P*4<0.001, *P*5<0.001, *P*6<0.001
Mast cell	18.7±11.01	17.1±0.56	16.8±7.61	8.3±6.91	0.025	*P*1=0.998, *P*2=0.998, *P*3=0.130, *P*4=1.00, *P*5=0.018, *P*6=0.101
VEGF	46.0±40.74	43.5±43.33	39.0±43.25	23.0±13.16	0.521	---------
MMP9	184.0±102.98	74.0±16.47	64.0±14.3	49.0±20.11	<0.001	*P*1=0.563, *P*2<0.001, *P*3<0.001, *P*4=0.699, *P*5=0.336, *P*6<0.001

***:** Significantly higher than their corresponding in the other subgroups; **†:** Significantly lower than their corresponding in the other subgroups; ***P*1:** b Vs c, ***P*2:** b Vs d, ***P*3:** b Vs e, ***P*4:** c Vs d, ***P*5:** c Vs e, ***P*6:** d Vs e.

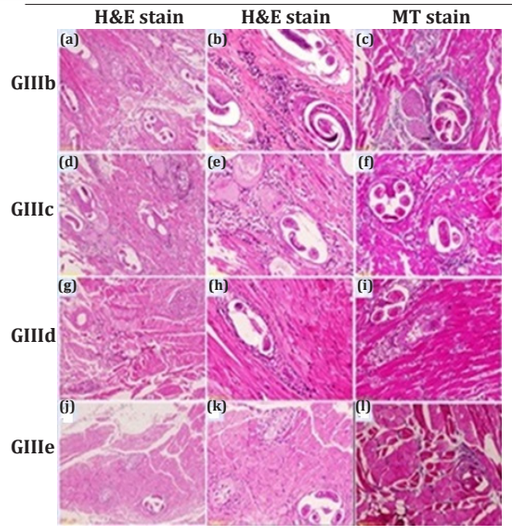

Fig. 3. The histopathological changes in the late treated muscular phase in the studied subgroups. **a)** Marked dense infiltrate by *T. spiralis* larvae in the infected subgroup (H&E x40). **b)** Marked inflammatory infiltrate with little destruction of the larva in infected subgroup (H&E x100). **c)** Thick capsule around the larva in infected subgroup (MT x100). **d)** Moderate number of *T. spiralis* larval infiltration in ABZ-treated subgroup (H&E x40). **e)** Moderate inflammatory infiltrate with mild lysis of the larva in ABZ-treated subgroup (H&E x100). **f)** Mild thinning of the capsule of *T. spiralis* larva in ABZ-treated subgroup (MT x100). **g)** Low number and size of *T. spiralis* larva in Cur-Nano treated subgroup (H&E x40). **h)** Mild inflammatory infiltrate associated with marked lysis of the larva in Cur-Nano treated subgroup (H&E x100). **i)** Thinning of the larval capsule in Cur-Nano treated subgroup (MT x100). **j)** Few numbers of *T. spiralis* larvae in ABZ/Cur-Nano treated subgroup (H&E x40). **k)** Minimal inflammatory infiltrate and marked lysis of larva in ABZ/Cur-Nano treated subgroup (H&E x100). **l)** Marked thinning of the larval capsule in ABZ/Cur-Nano treated subgroup (MT x100). **MT:** Masson trichrome.

treated subgroups compared to the infected non-treated subgroup (51.90±3.07) with *P*<0.001 for all. The eosinophils count was significantly low in GIIIe (10.00±0.66) followed by GIIId (14.80±0.91) and then GIIIc (21.20±1.39) and P<0.001 for all. However, the mast cells count showed no significant difference between the treated subgroups; GIIIc (17.10±0.56), GIIId (16.80±7.61) and GIIIe (8.30±6.91) compared to GIIIb (18.70±11.01). Meanwhile, the only significant difference was observed between ABZ-treated (GIIIc) and Cur-Nano/ABZ treated (GIIIe) subgroups regarding mast cells count (*P*=0.018) (Table 4).

The immunohistochemical results of VEGF and MMP 9 expression in the early and late treated muscular phases: In the early treated (13th dpi) muscle phase, there was a significant low VEGF expression in the Cur-Nano/ABZ treated subgroup GIIe (19.00±22.94), ABZ-treated subgroup GIIc (31.50±36.28), and Cur-Nano treated subgroup GIId (40.50±38.67) compared to infected non-treated group GIIb (131.50±81.31), (*P*=0.010, *P*=0.022, and *P*=0.050, respectively). However, there was no significant difference between GIIc, GIId and GIIe regarding VEGF expression (Fig. 4 a, c, e, g). Similarly, there was a significant

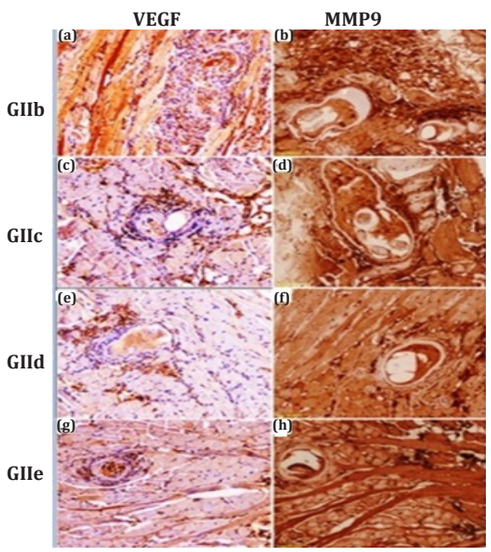

Fig. 4. The immunohistochemical expression of VEGF and MMP9 in the early treated muscular phase. **a)** High expression of VEGF in infected subgroup (IHC x100). **b)** High expression of MMP9 in infected subgroup (IHC x100). **c)** Mild expression of VEGF in ABZ-treated subgroup (IHC x100). **d)** Moderate expression of MMP9 in ABZ-treated subgroup (IHC x100). **e)** Moderate expression of VEGF in Cur-Nano treated subgroup (IHC x100). **f)** Mild expression of MMP9 in Cur-Nano treated subgroup (IHC x100). **g)** Mild expression of VEGF in ABZ/Cur-Nano treated subgroup (IHC x100) **h)** Mild expression of MMP9 in ABZ/Cur-Nano treated subgroup (IHC x100).

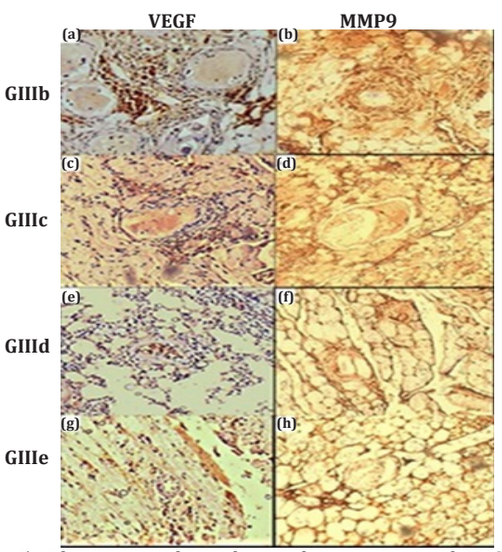

Fig. 5. The immunohistochemical expression of VEGF and MMP9 in the late treated muscular phase. **a)** High expression of VEGF in infected subgroup (IHC x100). **b)** High expression of MMP9 in infected subgroup (IHC x100). **c)** Moderate expression of VEGF in ABZ-treated subgroup (IHC x100). **d)** Moderate expression of MMP9 in ABZ-treated subgroup (IHC x100). **e)** Mild expression of VEGF in Cur-Nano treated subgroup (IHC x100). **f)** Mild expression of MMP9 in Cur-Nano treated subgroup (IHC x100). **g)** Mild expression of VEGF in ABZ/Cur-Nano treated subgroup (IHC x100). **h)** Mild expression of MMP9 in ABZ/Cur-Nano treated subgroup (IHC x100).

low MMP9 expression in GIIe (45.00±51.20), GIId (52.50±47.15), and GIIc (71.00±67.11) compared to GIIb (161.00±87.86) (P<0.001, P=0.001, and P=0.004, respectively). However, there was no significant difference between GIIc, GIId and GIIe regarding MMP9 expression (Fig. 4 b, d, f, h, and table 3).

In the late treated (31st dpi) muscle phase, there was no significant difference in VEGF expression between the treated and the infected non-treated subgroups (Fig. 5 a, c, e, g). However, there was a significant difference regarding MMP9 expression between the Cur-Nano treated GIIId and the Cur-Nano/ABZ treated GIIIe compared to the infected non-treated subgroup GIIIb (P<0.001, and P<0.001, respectively). In addition, there was a significantly low expression of MMP9 in the GIIIe compared to GIIId (P<0.001) (Fig. 5 b, d, f, h, and table 4).

Comparing the drug's effectiveness on the muscle phase concerning the day of administration: Regarding ABZ treatment, there was significant degradation and lysis of larvae during the early treated muscular phase (GIIc) compared to the late treated phase (GIIIc) (P=0.043). However, there was no significant difference regarding the inflammatory response or muscular degenerative changes during both phases. The expression of VEGF was decreased significantly during the early treated GIIc compared to the late treated GIIIc (P<0.001). There was no significant difference regarding MMP9 expression during both phases.

Regarding Cur-Nano treatment, there was a significance regarding the number of larvae during the late treated GIIId compared to the early treated GIId (P<0.001). Similarly, the impact was significantly observed in the degradation and lysis of larvae during the late treated muscle phase compared to the early treated phase (P<0.001). On the other hand, there was no significant difference regarding the inflammatory response or muscular degenerative changes during both phases. In addition, there was no significant difference regarding VEGF and MMP9 expression during both phases.

Table 5. Comparing the drug's effectiveness on histopathological changes during the mus¬cle phase in relation to the day of administration in each subgroup.

Variable	ABZ		Cur-Nano		Cur-Nano/ABZ	
	Early (GIIc) No. (%)	Late (GIIIc) No. (%)	Early (GIId) No. (%)	Late (GIIId) No. (%)	Early (GIIe) No. (%)	Late (GIIIe) No. (%)
Inflammation						
Mild	7 (70.0)	3 (30.0)	2 (20.0)	7 (70.0)	9 (90.0)	10 (100.0)
Moderate	3 (30.0)	7 (70.0)	8 (80.0)	3 (30.0)	1 (10.0)	0 (0.0)
***P* value**	0.074		0.07		1.00	
Capsule thinning						
Mild	2 (20.0)	0 (0.0)	8 (80.0)	0 (0.0)	0 (0.0)	0 (0.0)
Moderate	8 (80.0)	6 (60.0)	2 (20.0)	6 (60.0)	2 (20.0)	2 (20.0)
Marked	0 (0.0)	4 (40.0)	0 (0.0)	4 (40.0)	8 (80.0)	8 (80.0)
***P* value**	0.043		<0.001		1.00	
Degradation						
Mild	2 (20.0)	0 (0.0)	9 (90.0)	0 (0.0)	0 (0.0)	0 (0.0)
Moderate	8 (80.0)	6 (60.0)	1 (10.0)	5 (50.0)	1 (10.0)	3 (30.0)
Marked	0 (0.0)	4 (40.0)	0 (0.0)	5 (50.0)	9 (90.0)	7 (70.0)
***P* value**	0.043		<0.001		0.582	
Muscle by MT						
Mild	4 (40.0)	3 (30.0)	4 (40.0)	8 (80.0)	6 (60.0)	10 (100.0)
Moderate	6 (60.0)	7 (70.0)	6 (60.0)	2 (20.0)	4 (40.0)	0 (00.0)
***P* value**	1.00		0.170		0.087	
No. of larva	19.8±1.75	24.2±6.40	33.2± 9.30	18.8±1.22	16.8±1.22	10.7±1.56
***P* value**	0.013		<0.001		0.04	
Eosinophils	18.8±0.91	21.2±1.39	31.9±2.64	14.8±0.91	4.8±0.78	10.0±0.66
***P* value**	<0.001		<0.001		<0.001	
Mast cells	3.7±1.56	17.1±0.56	2.6±2.22	16.8±7.61	4.0±3.68	8.3±6.91
***P* value**	<0.001		<0.001		0.098	
VEGF	31.5±36.28	43.5±43.33	40.5±48.67	39.0±43.25	19.0±22.94	23.0± 13.16
***P* value**	<0.001		0.943		0.638	
MMP9	71.0± 67.12	74.0±16.47	52.5±47.16	64.0±14.3	45.0±25.82	45.0±25.82
***P* value**	0.908		0.657		0.877	

*: Significantly higher than their corresponding in the other groups.

Regarding Cur-Nano/ABZ treatment, there was a significance regarding the number of larvae during the late treated muscle phase (GIIIe) compared to the early phase (GIIe) (P<0.001). However, there was no significant difference between both phases regarding the degradation and lysis of larvae. Similarly, there was no significant difference regarding the inflammatory response or muscular degenerative changes during both phases. There was also no significant difference regarding VEGF and MMP9 expression during both phases (Table 5).

Serum biochemical results: For the early and late treated muscle groups, the mean CK level was 46.02±2.96 and 47.35±4.61 in subgroup GIIa and GIIIa (negative control), respectively. While the level was 363.06±0.12 and 364.16±0.36 in the GIIb and GIIIb (positive control subgroups), respectively, followed by ABZ (208.19±0.81, and 210.39±1.48, respectively), then Cur-Nano (196.00±1.84, and 127.84±1.83, respectively) and the lowest level was 183.87±1.12 and 117.74 ± 1.37, respectively in the combined treated subgroups. Each subgroup was significantly different from all the others (P<0.001 for each subgroup) (Table 6).

Regarding MMP level in the early muscular group (GII), it was 92.73±0.48, 93.18±0.14 in subgroup IIb (infected non-treated), followed by subgroup IIc (77.89±3.33), then subgroup IId (71.39±0.56) and subgroup IIe (61.59±1.41). Meanwhile, it was 52.23±2.52, 51.64±2.69 in subgroup IIa (normal control). Each subgroup was significantly different from the others (P<0.001 for each subgroup). For the late muscular group (GIII), the mean MMP level was significantly high in the subgroup IIIb (infected non-treated), followed by subgroups IIIc, IIId and IIIe (93.18±0.14, 80.92±0.34, 67.09±0.85, and 54.28±0.59, respectively). While it was 51.64±2.69 in subgroup IIIa (normal control) (P<0.001). Each subgroup was significantly different from all the others (P<0.001 for each subgroup), except for the subgroups IIIe and IIIa where there was no significant difference from each other (Table 6).

Regarding the mean TAC level in the early (GII) and late muscular (GIII) groups, it was significantly high in the subgroup e (4.84±0.21, and 8.07±0.13, respectively), followed by subgroup d (4.05±0.17, and 6.98±0.18. respectively) then subgroup c (2.84±0.31, and 1.93±0.16, respectively), while it was 1.15±0.06, and 1.09±0.02, respectively in subgroup b (infected control) and 1.30±0.04, and 1.27±0.06, respectively in subgroup a (normal control). Each subgroup was significantly different from all the others (P<0.001 for each subgroup) (Table 6).

Furthermore, the mean MDA level in the early (GII) and late muscular (GIII) groups were significantly high in the subgroup b (infected control) (5.78±0.04, and 5.86±0.05, respectively), followed by subgroup c (4.92±0.23, and 4.15±0.19, respectively), subgroup d (3.12±0.10, and 1.95±0.08, respectively) and subgroup e (2.67±0.35, and 1.50±0.02, respectively). While it was 1.12±0.03, and 1.14±0.04, respectively in subgroup a (normal control). Each subgroup was significantly different from all the others (P<0.001) (Table 6).

Table 6. Serum investigations during muscular phase among the different subgroups.

Groups	CK (IU/L) Mean±SD	MMP (mmol/L) Mean±SD	TAC (mmol/L) Mean±SD	MDA (mmol/L) Mean±SD
Early muscular (GII)				
IIa	46.02 ± 2.96	52.23 ± 2.52	1.30 ± 0.04	1.12 ± 0.03
IIb	363.06 ± 0.12	92.73 ± 0.48	1.15 ± 0.06	5.78 ± 0.04
IIc	208.19 ± 0.81	77.89 ± 3.33	2.84 ± 0.31	4.92 ± 0.23
IId	196.00 ± 1.84	71.39 ± 0.56	4.05 ± 0.17	3.12 ± 0.10
IIe	183.87 ± 1.12	61.59 ± 1.41	4.84 ± 0.21	2.67 ± 0.35
***P* value**	<0.001	<0.001	<0.001	<0.001
Post-Hoc	*P*1<0.001, *P*2<0.001, *P*3<0.001, *P*4<0.001, *P*5<0.001, *P*6<0.001, *P*7<0.001, *P*8<0.001, *P*9<0.001, *P*10<0.001	*P*1<0.001, *P*2<0.001, *P*3<0.001, *P*4<0.001, *P*5<0.001, *P*6<0.001, *P*7<0.001, *P*8<0.001, *P*9<0.001, *P*10<0.001	*P*1<0.001, *P*2<0.001, *P*3<0.001, *P*4<0.001, *P*5<0.001, *P*6<0.001, *P*7<0.001, *P*8<0.001, *P*9<0.001, *P*10<0.001	*P*1<0.001, *P*2<0.001, *P*3<0.001, *P*4<0.001, *P*5<0.001, *P*6<0.001, *P*7<0.001, *P*8<0.001, *P*9<0.001, *P*10=0.028
Late muscular (GIII)				
IIIa	47.35 ± 4.61	51.64 ± 2.69	1.27 ± 0.06	1.14 ± 0.04
IIIb	364.16 ± 0.36	93.18 ± 0.14	1.09 ± 0.02	5.86 ± 0.05
IIIc	210.39 ± 1.48	80.92 ± 0.34	1.93 ± 0.16	4.15 ± 0.19
IIId	127.84 ± 1.83	67.09 ± 0.85	6.98 ± 0.18	1.95 ± 0.08
IIIe	117.74 ± 1.37	54.28 ± 0.59	8.07 ± 0.13	1.50 ± 0.02
***P* value**	<0.001	<0.001	<0.001	<0.001
Post-Hoc	*P*1<0.001, *P*2<0.001, *P*3<0.001, *P*4<0.001, *P*5<0.001, *P*6<0.001, *P*7<0.001, *P*8<0.001, *P*9<0.001, *P*10<0.001	*P*1<0.001, *P*2<0.001, *P*3<0.001, *P*4=0.121, *P*5<0.001, *P*6<0.001, *P*7<0.001, *P*8<0.001, *P*9<0.001, *P*10<0.001	*P*1<0.001, *P*2<0.001, *P*3<0.001, *P*4<0.001, *P*5<0.001, *P*6<0.001, *P*7<0.001, *P*8<0.001, *P*9<0.001, *P*10<0.001	*P*1<0.001, *P*2<0.001 *P*3<0.001, *P*4<0.001 *P*5<0.001, *P*6<0.001 *P*7<0.001, *P*8<0.001 *P*9<0.001, *P*10<0.001

***P*1:** a Vs b; ***P*2:** a Vs c; ***P*3:** a Vs d; ***P*4:** a Vs e; ***P*5:** b Vs c; ***P*6:** b Vs d; ***P*7:** b Vs e; ***P*8:** c Vs d; ***P*9:** c Vs e; ***P*10:** d Vs e.

DISCUSSION

Lack of a fully effective medicine has restrained medical therapy of trichinosis. However, it was noted that the treatment for trichinosis was most beneficial when chemotherapy was started early[41]. Therefore, the use of Cur and Cur-loaded nanoparticles would be crucial for its therapeutic uses since they increase its effectiveness against a variety of microbial diseases and parasites[42]. The present work's primary objective was to study the trichinecidal effect of Cur-Nano alone or in combination with ABZ on enteral and parenteral phases of *T. spiralis* infected mice.

In the present study, ABZ/Cur-Nano combined therapy showed the lowest worm count and the highest reduction rate. Similar results were reported by Hamed *et al*.[43] who showed that the groups taking albendazole alone or in conjunction with Cur had the lowest intestinal worm. Besides, Elmehy *et al*.[44] and Nassef *et al*.[45] reported that combined treatment of both ABZ and mefloquine, and chitosan nanoparticles loaded with a full dose of ABZ, respectively resulted in a notable decrease in the average number of adult *T. spiralis* worms in the infected mice. Herein, reduction in larval count in all treated subgroups during the muscle phases (early and late treated) was observed. These results are consistent with those of Attia *et al*.[3] who found that ABZ had a reduced efficiency against encysted larvae (65.2% reduction). Additionally, earlier studies indicated substantially lower efficacies of ABZ against encysted muscle larvae[46,19]. This is due to limited bioavailability, a high degree of resistance and limited effectiveness against encysted *T. spiralis* larvae[14]. The current lethal effect of Cur-Nano on encysted larvae of *T. spiralis* is consistent with the results of Hamed *et al*.[43], who reported reduced larval count during the muscle phase with the highest reduction rate of larvae (80.2%) in the subgroup treated by Cur-Nano. In addition, Elguindy *et al*.[9] evaluated the anti-nematode activity of Cur against *T. spiralis* and found that in mice sacrificed 35 dpi, the muscle larval count was decreased by 53%. In addition, Cur has anti-angiogenic properties[47], which increase its ability of lowering the muscle larval counts by making the skeletal muscle cells less hospitable to *Trichinella* larvae, depriving the larvae of their nourishment, resulting in the accumulation of their wastes, and ultimately leading to their death. The same results were reported by multiple studies of Cur-Nano against a variety of parasites. Several studies showed that nano-formulation of Cur exhibited significant efficacy against toxoplasmosis[20], malignant malaria[48], leishmanicidal activity[49], and ovicidal activity against Schistosoma ova settled in the intestinal wall[50].

Interestingly, combination therapy seems to have higher therapeutic efficacy than individual treatments. It results in a maximum reduction of the intestinal and muscular phases (99.32 % and 95.94%, respectively). The significant parasiticidal effects are likely attributed to the dual action of ABZ and Cur-Nano against *T. spiralis* adult worms and muscle larvae. Khedr *et al*.[51] revealed similar findings demonstrating that ABZ was efficacious but that its combination with Cur nano-emulsion significantly enhanced its effectiveness against adult worms and muscle larvae and reduced disease in both models.

The histological results of the current study during the intestinal phase revealed severe tissue damage that may be attributed to increased levels of reactive oxygen species (ROS) and inflammatory cells[52]. Similar results were reported by Hamed *et al*.[43], who revealed marked improvement of histopathological alterations in mice groups infected with *T. spiralis* when treated by Cur-Nano, compared to the control group, and ABZ-administered infected group. In addition, our previous study on trichinosis showed that Cur-Nano had more significant effects on pathogenesis and inflammation with notable improvement in different mice organs[22]. Moreover, these results are parallel to previous studies[19,45] using different nanoparticles in trichinosis. Both studies reported marked improvement of the intestinal histopathological changes and degeneration of encysted larvae with minimal pathologic changes of infected skeletal muscles in the groups treated by chitosan nanoparticles loaded with ABZ. In addition, EL-Melegy *et al*.[32] demonstrated a significant decrease in the inflammatory response with restoration of the almost normal appearance of the skeletal muscle fibers in the group of mebendazole-loaded silver nanoparticles.

Trichinosis is a well-known parasitic disease that exhibits the eosinophilic response. Eosinophils have been demonstrated to display a harmful effect during primary infection of *T. spiralis* through antibody-dependent cellular cytotoxicity. Eosinophils promote larval growth by activating the IL-4/STAT6 signaling pathways, which reduces local inflammation and improves larval feeding and metabolism[53]. According to earlier research, the delayed development of intestinal mast cells and the subsequent inflammation are the main causes of *T. spiralis* infection persistence[54]. Herein, compared to the infected non-treated subgroup, eosinophil and mast cells levels were noticeably decreased in all treated subgroups. Interestingly, a key pharmacological activity of Cur is a potent immunomodulatory property, which arises from its strong interactions with various types of immune cells such as epithelial cells, basophils, mast cells, neutrophils, eosinophils, and also T cells, leading to the regulation of pathologic immune responses. Besides, Cur also reduces the inflammation by inhibiting the production of IL-4 and TNF-α, thereby ameliorating the recruitment of neutrophils and eosinophils[55].

On comparison of early and late treated muscle phases, there was a significance regarding the number of larvae in the late treated muscle phase in Cur-Nano and ABZ/Cur-Nano treated subgroups. Additionally, all treated subgroups showed significant degradation and lysis of larvae during the late treated muscular phase compared to the early treated phase. However, there was no significant difference regarding the inflammatory response or muscular degenerative changes during both phases. Both early and late treatment gave good results with significant difference in the late phase (on the 31th dpi). Against our results, Basyoni and El-Sabaa[56] used Ivermectin and myrrh for controlling *T. spiralis* and showed that early muscular treatment at day 15 dpi is more effective than late muscular treatment at day 35 dpi, and this result may be contributed to the medication used.

In this study, ABZ showed antilarval effect with slightly better results when used earlier during the muscular phase (74.34% on 13th dpi and 70.51% on 31st dpi). On the other hand, Cur-Nano had antilarval effect in both early and late treatment with considerably enhanced results in the late phase (64.88% on 13th dpi and 85.26% on 31st dpi) which could be explained by the multiple Cur bioactive properties that affect both the encysted larvae and the host cells. When combined treatment was applied it was found to manifest good results both early and late. Unexpectedly, the reduction rate was higher in the late phase (89.11% on 13th dpi and 95.94% on 31st dpi) which could be understood in view of combining the action of both medications due to increased biological activity and various antiparasitic mechanisms.

In this study, there was an improvement in serum CK level in all treated subgroups with marked improvement in the combined late ABZ/Cur-Nano treated subgroups. Administration of Cur-Nano significantly reduces CK because Cur has a membrane-stabilizing action by inhibiting the release of beta-glucuronidase from nuclei, mitochondria, lysosomes, and microsomes[57]. These results were in accordance with Boarescu *et al*.[57] who stated that Cur-Nano prevented elevation of CK. Besides, EL-Melegy *et al*.[32] observed a decrease in CK level in all treated mice compared to the infected control group, with a significant decrease ($P \leq 0.0001$) in the treated group using mebendazole-loaded silver nanoparticles compared to other treated groups.

The TAC and MDA concentration changes are useful indicators to assess oxidative stress. Herein, the improvement of TAC level was recorded in all treated subgroups, with more significant results obtained in Cur-Nano treated subgroups. In addition, combined ABZ/Cur-Nano and Cur-Nano were effective in reducing serum MDA levels during both early and late treated muscle phases. It was reported that Cur modulates oxidative stress[58]. It might exert its effects via causing a decrease in ROS production with subsequent rise in TAC levels[59]. Furthermore, Cur administration could dramatically lower MDA because it can reduce lipid peroxidation brought on by hydrogen peroxide and inhibit nitric oxide synthase activity thus lowering nitric oxide generation[60]. Consequently, Cur antioxidant properties can participate in its antiparasitic action[61]. Boarescu *et al*.[57] demonstrated that Cur-Nano dramatically improved antioxidative markers (TAC) and decreased blood levels of oxidative stress markers (MDA) in diabetic rats with drug-induced acute myocardial infarction. Owing to Cur being administered in encapsulated nanocarriers that increases its antioxidant capabilities, MDA levels have been lowered and TAC levels have increased.

The results of our study showed a decrease in the serum level and tissue expression of MMP9 in ABZ/Cur-Nano treated subgroups. These findings were supported by Boarescu *et al*.[57] who observed that Cur-Nano can greatly raise TAC and lower MMP2 and MMP9 levels in rats after myocardial infarction. Treatment with Cur inhibits MMP2 and MMP9 due to its powerful antioxidant effect[62].

Regarding VEGF, the infected non-treated subgroups showed local positive expressions. In agreement with our results, Othman *et al*.[12] revealed that VEGF was expressed in muscle fibers of *T. spiralis*-infected mice; providing the essential blood supply to nourish and maintain *T. spiralis* larval stages within these distressed muscles. In addition, there was a significant low expression VEGF in ABZ/Cur-Nano treated subgroups followed by Cur-Nano treated subgroups. Similarly, Fu *et al*.[63] demonstrated that Cur inhibits the expression of VEGF both in vitro and in vivo by acting on the VEGF receptor-2 pathway. Additionally, Giménez-Bastida *et al*.[64] showed that Cur inhibits VEGF, producing powerful antiangiogenic effects on microvascular endothelial cells isolated from the human intestine. These findings may offer a good understanding of the curative effects of Cur in illnesses like cancer and chronic inflammation, where pathological neovascularization is linked to an increased production of VEGF.

Trichinosis upregulates the angiogenic VEGF by inducing thymosin 4, which results in the development of blood vessels that maintain larval survival in the early stages of muscle infection. Angiogenesis is crucial for nurse cell formation and VEGF is an important signaling protein involved in vasculogenesis and angiogenesis[12]. As well, MMPs are well-known markers of angiogenesis as they control immunity and inflammation and are crucial enzymes for the breakdown of extracellular matrix[65]. Therefore, one of the hypothesized mechanisms

for the reduction of *T. spiralis* larval growth is the inhibition of angiogenesis[13] and by lowering VEGF and MMPs, Cur suppresses angiogenesis[47].

In conclusion, the results of this study proved that nanoparticles are effective delivery system for Cur since it had antiparasitic action against trichinosis with advantageous outcomes in the muscle phase. It induced its effect through antioxidant alterations in TAC and MDA along with inhibition of angiogenesis by reduction of VEGF and MMP. However, in the intestinal phase, ABZ has better effect than Cur-Nano. Furthermore, the synergistic activity of both drugs (ABZ/Cur-Nano treatment) provides the best results in both intestinal and muscular phases due to increased biological activity and multiple antiparasitic mechanisms. Therefore, combined therapy may be a promising alternative treatment for trichinosis.

Author contribution: Atia A proposed the study topic. Atia A, Abokhalil N and Abo-Hussien N designed the study and contributed in writing the manuscript. Sweed D performed the pathology evaluation. Mandour S performed the biochemical assessment, and Soliman S statistically analyzed and interpreted the data. Atia A and Abokhalil N revised the article. All authors read through and approved the final manuscript.

Conflicts of interest: None.

Funding statement: There was no specific grant for this research from a funding organization in the private or nonprofit sectors.

REFERENCES

1. Muñoz-Carrillo JL, Muñoz-López JL, Muñoz-Escobedo JJ, Maldonado-Tapia C, Gutiérrez-Coronado O, Contreras-Cordero JF, *et al*. Therapeutic effects of resiniferatoxin related with immunological responses for intestinal inflammation in trichinellosis. Korean J Parasitol 2017; 55(6):587-599.
2. Yadav A, Rafiqi SI, Yadav V, Godara R, Katoch R. An overview on under researched and neglected emerging parasitic zoonosis. Indian J Com 2021; 23(2):125-134.
3. Attia RA, Mahmoud AE, Farrag HM, Makboul R, Mohamed ME, Ibraheim Z. Effect of myrrh and thyme on *Trichinella spiralis* enteral and parenteral phases width inducible nitric oxide expression in mice. Mem Inst Oswaldo Cruz 2015; 110(8):1035-1041.
4. Wang ZQ, Shi YL, Liu RD, Jiang P, Guan YY, Chen YD, *et al*. New insights on serodiagnosis of trichinellosis during window period: Early diagnostic antigens from *Trichinella spiralis* intestinal worms. Infect Dis Poverty 2017; 6(1):41.
5. Yan J, Huang S, Lu F. Galectin-receptor interactions regulate cardiac pathology Caused by *Trichinella spiralis* infection. Front Immunol 2021; 12:639260.
6. Grencis RK, Humphreys NE, Bancroft AJ. Immunity to gastrointestinal nematodes: Mechanisms and myths. Immunol Rev 2014; 260:183-205.
7. Javkar T, Hughes KR, Sablitzky F, Behnke JM, Mahida YR. Slow cycling intestinal stem cell and Paneth cell responses to *Trichinella spiralis* infection. Parasitol Int 2020;74:101923.
8. Wang A, Liu X, Heckmann A, Caignard G, Vitour D, Hirchaud E, *et al*. A *Trichinella spiralis* newborn larvae specific protein, Ts NBL1, interacts with host's cell vimentin. Parasitol Res 2022; 121:1369–1378.
9. Elguindy DA, Ashour DS, Shamloula MM, Aboul Assad IA. Preliminary study on the role of toll-like receptor-4 antagonist in treatment of *Trichinella spiralis* infection. Tanta Med J 2019; 47:52–61.
10. Park MK, Cho MK, Kang SA, Kim BY, Yu HS. The induction of the collagen capsule synthesis by *Trichinella spiralis* is closely related to protease-activated receptor 2. Vet Parasitol 2016; 230:56–61.
11. Park MK, Kim HJ, Cho MK, Kang SA, Park SY, Jang SB, *et al*. Identification of a host collagen inducing factor from the excretory secretory proteins of *Trichinella spiralis*. PLoS Negl Trop Dis 2018; 12(11): e0006516.
12. Othman AA, Abou Rayia DM, Ashour DS, Saied EM, Zineldeen DH, El-Ebiary AA. Atorvastatin and metformin administration modulates experimental *Trichinella spiralis* infection. Parasitol Int 2016; 65(2):105-112.
13. Ock MS, Cha HJ, Choi YH. Verifiable hypotheses for thymosin β4-dependent and -independent angiogenic induction of *Trichinella spiralis*-triggered nurse cell formation, Int J Mol Sci 2013;14:23492–23498.
14. Garcia A, Leonardi D, Vasconi MD, Hinrichsen LI, Lamas MC. Characterization of albendazole- randomly methylated- β-cyclodextrin inclusion complex and in vivo evaluation of its anthelminthic activity in a murine model of trichinellosis. PLoS One 2014; 9(11): e113296.
15. Rai M, Ingle AP, Pandit R, Paralikar P, Anasane N, Santos CAD. Curcumin and curcumin-loaded nanoparticles: Antipathogenic and antiparasitic activities. Expert Rev Anti Infect Ther 2020; 18(4): 367-379.
16. Asadpoura M, Namazia F, Razavia SM, Nazifi S. Comparative efficacy of curcumin and paromomycin against Cryptosporidium parvum infection in a BALB/c model. Vet Parasitol 2018; 250: 7–14.
17. Cervantes-Valencia ME, Hermosilla C, Alcalá-Canto Y, Tapia G, Taubert A, Silva L M. Antiparasitic efficacy of curcumin against Besnoitia besnoiti tachyzoites in vitro. Front Vet Sci. 2019; 5:333.
18. Dende C, Meena J, Nagarajan P, Nagaraj VA, Panda AK, Padmanaban G. Nanocurcumin is superior to native curcumin in preventing degenerative changes in Experimental Cerebral Malaria. Sci Rep 2017; 7(1):10062.
19. Nassef NE, Moharm IM, Atia AF, Brakat RM, Abo-Hussien NM, Shamseldeen AM. Therapeutic efficacy of chitosan nanoparticles loaded with albendazole on parenteral phase of experimental trichinellosis. J Egypt Soc Parasitol (JESP) 2019; 49(2): 301-311.
20. Azami SJ, Teimouri A, Keshavarz H, Amani A, Esmaeili F, Hasanpour H, *et al*. Curcumin nanoemulsion as a novel chemical for the treatment of acute and chronic

toxoplasmosis in mice. Int J Nanomedicine 2018; 13: 7363–7374.
21. Devara RK, Mohammad HUR, Rambabu B, Aukunuru J, Habibuddin M. Preparation, optimization and evaluation of intravenous curcumin nanosuspension intended to treat liver fibrosis. Turk J Pharm Sci 2015; 12, (2): 207-220.
22. Atia AF, Abokhalil NA, Sweed DM, Moaz IM, Abo-Hussien NM. Curcumin nanoparticles versus curcumin in amelioration of inflammatory and pathological changes during the migratory phase of murine trichinellosis. J Egypt Soc Parasitol (JESP) 2021; 51(2): 239-256.
23. Denham DA, Martinez AR. Studies with methyridine and *Trichinella spiralis*. 2. The use of drugs to study the rate of larval production in mice. J Helminthol 1970; 44: 357-363.
24. Huang H, Yao J, Liu K, Yang W, Wang G, Shi C, *et al*. Sanguinarine has anthelmintic activity against the enteral and parenteral phases of *Trichinella* infection in experimentally infected mice. Acta Trop 2020; 201:105226.
25. Yadav AK, Temjenmongla. Efficacy of *Lasia spinosa* leaf extract in treating mice infected with *Trichinella spiralis*. Parasitol Res 2012; 110:493-498.
26. Issa RM, El-Arousy MH, Abd EI-Aal AA. Albendazole: a study of its effect on experimental *Trichinella spiralis* infection in rats. Egypt J Med Sci 1998; 19:281-290.
27. Ashour DS, Abou Rayia DM, Saad AE, El-Bakary RH. Nitazoxanide anthelminthic activity against the enteral and parenteral phases of trichinellosis in experimentally infected rats. Exp Parasitol 2016; 170:28-35.
28. Denham DA. Studies with methyridine and *Trichinella spiralis*. I. Effect upon the intestinal phase in mice. Exp Parasitol 1965; 17(1):10-14.
29. Bancroft JD, Gamble M. Theory and practice of histological techniques. Churchill Livingstone, London. 2008.
30. Blum LK, Mohanan S, Fabre MV, Yafawi RE, Appleton JA. Intestinal infection with *Trichinella spiralis* induces distinct, regional immune responses. Vet Parasitol 2013; 194(2-4):101-105.
31. Saracino MP, Vila CC, Cohen M, Gentilini MV, Falduto GH, *et al*. Cellular and molecular changes and immune response in the intestinal mucosa during *Trichinella spiralis* early infection in rats. Parasit Vectors 2020; 13 (1):505.
32. El-Melegy MA, Ghoneim NS, El-Dien NMN, Rizk MS. Silver nano particles improve the therapeutic effect of mebendazole treatment during the muscular phase of experimental trichinellosis. J Am Sci 2019; 15(5). DOI:10.7537/marsjas150519.06.
33. Cheng G, Zhang Z, Wang Y, Zao Y, Wang R, Gao M, *et al*. *Trichinella spiralis*-secreted products promote collagen capsule formation through TGF-β1/Smad3 pathway. Int J Mol Sci 2023; 24(19):15003.
34. Ding J, Bai X, Wang X, Shi H, Cai X, *et al*. Immune cell responses and cytokine profile in intestines of mice infected with *Trichinella spiralis*. Front Microbiol 2017; 8:2069.
35. Shojaeian S, Lay NM, Zarnani AH. Detection systems in immunohistochemistry. In Immunohistochemistry: The Ageless Biotechnology. London 2018: Intech Open.
36. Pu X, Storr SJ, Zhang Y, Rakha EA, Green AR, Ellis IO, *et al*. Caspase-3 and caspase-8 expression in breast cancer: Caspase-3 is associated with survival. Apoptosis 2017; 22:357–368.
37. Kopp J, Loos B, Spilker G, Horch RE. Correlation between serum creatinine kinase levels and extent of muscle damage in electrical burns. Burns 2004; 30:680–683.
38. Shibahara H, Suzuki T, Kikuchi K, Hirano Y, Suzuki M. Serum matrix metalloproteinase and tTissue inhibitor of metalloproteinase concentrations in infertile women achieved pregnancy following IVF-ET. Am J Reprod Immunol 2005; 54(4):186-192.
39. Malik UU, Siddiqui IA, Hashim Z, Zarina S. Measurement of serum paraoxonase activity and MDA concentrations in patients suffering with oral squamous cell carcinoma. Clin Chim Acta 2014; 430:38–42.
40. Emin S, Yordanova K, Dimov D, Ilieva V, Koychev A, *et al*. Total antioxidant capacity of plasma determined as ferrous reducing ability of plasma in patients with COPD. Trakia J Sci 2010; 8:205–213.
41. Pozio E, Ludovisi A, Pezzotti P, Bruschi F, Gómez-Morales MA. Retrospective analysis of hospital discharge records for cases of trichinellosis does not allow evaluation of disease burden in Italy. Parasite 2019; 26:42-46.
42. No DS, Algburi A, Huynh P, Moret A, Ringard M, Comito N, *et al*. Antimicrobial efficacy of curcumin nanoparticles against Listeria monocytogenes is mediated by surface charge. J Food Safe 2017; 37(4):e12353.
43. Hamed AMR, Abdel-Shafi IR, Elsayed MDA, Mahfoz AM, Tawfeek SE, Abdeltawab MSA. Investigation of the effect of curcumin on oxidative stress, local infl- ammatory response, COX-2 expression, and microvessel density in *Trichinella spiralis* induced enteritis, myositis and myocarditis in mice. Helminthologia 2022; 59(1):18–36.
44. Elmehy DA, Abdelhai DI, Elkholy RA, Elkelany MM, Tahoon, DM, Elkholy RA, *et al*. Immunoprotective inference of experimental chronic *Trichinella spiralis* infection on house dust mites induced allergic airway remodeling. Acta Trop 2021; 220: 105934.
45. Nassef NE, Moharm IM, Atia AF, Brakat RM, Abo- Hussien NM, Shamseldeen AM. Therapeutic efficacy of chitosan nanoparticles and albendazole in intestinal murine trichinellosis. J Egypt Soc Parasitol (JESP) 2018; 48(3):493–502.
46. Codina AV, García A, Leonardi D, Vasconi MD, Di Masso RJ, Lamas MC, *et al*. Efficacy of albendazole: β-cyclodextrin citrate in the parenteral stage of *Trichinella spiralis* infection. Int J Biol Macromol 2015; 77:203-206.

47. Wang TY, Chen JX. Effects of curcumin on vessel formation insight into the pro-and antiangiogenesis of curcumin. Evid Based Complement Alternat Med 2019;2019:1390795 .
48. Ghosh A, Banerjee T, Bhandary S, Surolia A. Formulation of nanotized curcumin and demonstration of its antimalarial efficacy. Int J Nanomedicine 2014; 9:5373.
49. Tiwari B, Pahuja R, Kumar P, Rath SK, Gupta KC, Goyal N. Nanotized curcumin and Miltefosine, a potential combination for treatment of experimental visceral leishmaniasis. Antimicrob Agents Chemother 2017; 61 (3):e01169-16.
50. Mokbel KEM, Baiuomy IR, Sabry AEA, Mohammed MM, El-Dardiry MA. *In vivo* assessment of the antischistosomal activity of curcumin loaded nanoparticles versus praziquantel in the treatment of Schistosoma mansoni. Sci Rep 2020; 10(1):1–9.
51. Khedr SI, Gomaa MM, Mogahed NMFH, Gamea GA, Khodear GA, Sheta E, *et al*. *Trichinella spiralis*: A new parasitic target for curcumin nanoformulas in mice models. Parasitol Int 2023; 98:102810.
52. Othman AA, Shoheib ZS. Detrimental effects of geldanamycin on adults and larvae of *Trichinella spiralis*. Helminthologia 2016; 53(2):126–132.
53. Huang L, Beiting DP, Gebreselassie NG, Gagliardo LF, Ruyechan MC, Lee NA *et al*. Eosinophils and IL-4 support nematode growth coincident with an innate response to tissue injury. PLoS Pathog 2015;11(12):e1005347.
54. El-Dardiry MA, Abdel-Aal AA, Abdeltawab MS, El-Sherbini M, Hassan MA, Abdel-Aal AA, *et al*. Effect of mast cell stabilization on angiogenesis in primary and secondary experimental *Trichinella spiralis* infection. Parasit Vectors 2021; 14(1):1-13.
55. Haftcheshmeh SM, Mirhafez SR, Abedi M, Heydarlou H, Shakeri A, Mohammadi A, *et al*. Therapeutic potency of curcumin for allergic diseases: A focus on immunomodulatory actions. Biomed Pharmacother 2022; 154:113646.
56. Basyoni MM, El-Sabaa AAA. Therapeutic potential of myrrh and ivermectin against experimental *Trichinella spiralis* infection in mice. Korean J Parasitol 2013; 51(3):297.
57. Boarescu PM, Boarescu I, Bocșan IC, Gheban D, Bulboacă AE, Nicula C, *et al*. Antioxidant and anti-inflammatory effects of curcumin nanoparticles on drug-induced acute myocardial infarction in diabetic rats. Antioxidants (Basel) 2019; 8(10):504.
58. Eser A, Hizli D, Haltas H, Namuslu M, Kosus A, Kosus N, *et al*. Effects of curcumin on ovarian ischemia-reperfusion injury in a rat model. Biomed Rep 2015; 3(6):807-813.
59. Al–Rubaei ZM, Mohammad TU, Ali LK. Effects of local curcumin on oxidative stress and total antioxidant capacity in vivo study. Pak J Biol Sci 2014; 17:1237–1241.
60. Abrahams S, Haylett WL, Johnson G, Carr JA, Bardien S. Antioxidant effects of curcumin in models of neurodegeneration, aging, oxidative and nitrosative stress: A review. Neuroscience 2019; 406:1-21.
61. Mallo n, LAMAS J, Sueiro RA, Leiro JM. Molecular targets implicated in the antiparasitic and anti-inflammatory activity of the phytochemical curcumin in trichomoniasis. Molecules 2020; 25(22):5321.
62. Bulboacă AE, Porfire A, Bolboacă SD, Nicula CA, Feștilă DG, Roman A, *et al*. Protective effects of liposomal curcumin on oxidative stress/antioxidant imbalance, metalloproteinases 2 and-9, histological changes and renal function in experimental nephrotoxicity induced by gentamicin. Antioxidants (Basel) 2021; 10(2):325.
63. Fu Z, Chen X, Guan S, Yan Y, Lin H, Hua ZC. Curcumin inhibits angiogenesis and improves defective hematopoiesis induced by tumor-derived VEGF in tumor model through modulating VEGF- VEGFR2 signaling pathway. Oncotarget 2015; 6(23):19469–19482.
64. Giménez-Bastida JA, Ávila-Gálvez MÁ, Carmena-Bargueno M, Pérez-Sánchez H, Espín JC, González-Sarrías A. Physiologically relevant curcuminoids inhibit angiogenesis via VEGFR2 in human aortic endothelial cells. Food Chem Toxicol 2022; 166:113254.
65. Bruschi F, Bianchi C, Fornaro M, Naccarato G, Menicagli M, Gomez-Morales MA *et al*. Matrix metalloproteinase (MMP)-2 and MMP-9 as inflammation markers of *Trichinella spiralis* and *Trichinella pseudospiralis* infections in mice. Parasite Immunol 2014; 36(10):540-549.